INTERNATIONAL RESEARCH JOURNAL OF ENGINEERING & APPLIED SCIENCES
ISSN: 2322-0821(O)
ISSN: 2394-9910(P)
VOLUME 14 ISSUE 1
Jan 2026 - Mar 2026
www.irjeas.org

Research Article

Correlation Between Interplanetary Magnetic Field Fluctuations and Geomagnetic Activity during current solar cycle 25

V.K. Mishra[1*], Praveen Tyagi[2]

[1] Assistant Professor, Atal Bihari Vajpayee Hindi Vishwavidyalay, Bhopal
vkmishra74@yahoo.com
[2]Junior Research Fellow, Atal Bihari Vajpayee Hindi Vishwavidyalay, Bhopal

**Corresponding Author*: vkmishra74@yahoo.com

DOI–10.55083/irjeas.2026.v14i01002

Abstract: Understanding how variations in the interplanetary magnetic field (IMF) influence geomagnetic activity is essential for comprehending the interactions between the Sun and Earth. This study examines the quantitative relationship between IMF fluctuations and geomagnetic disturbances during Solar Cycle 25, considering both short-term variations and long-term trends. High-resolution data from near-Earth spacecraft, including measurements of IMF vector components and solar wind plasma parameters, were analyzed alongside global geomagnetic indices such as Dst and Kp. Statistical methods, including time-lagged cross-correlation and variance analysis, were applied to evaluate how interplanetary magnetic conditions affect geomagnetic responses throughout the solar cycle. Periods of intensified southward IMF ($B_z < 0$) and enhanced magnetic variability are strongly associated with increased geomagnetic activity. Correlation strengths fluctuate systematically over the solar cycle, reflecting changes in solar wind conditions and the large-scale configuration of the solar magnetic field. These findings offer updated insights into solar wind–magnetosphere coupling under current solar conditions and contribute to improved understanding and forecasting of space weather phenomena.

Keywords: Interplanetary magnetic field, geomagnetic activity, Solar Cycle 25, space weather, solar wind–magnetosphere coupling.

1. INTRODUCTION

Geomagnetic activity at Earth results from the complex interaction between the solar wind and the planet's magnetosphere. Among the factors influencing this interaction, the interplanetary magnetic field plays a crucial role by regulating the transfer of energy and momentum from the solar wind into near-Earth space. Variations in the IMF arise from processes on the solar surface, including coronal mass ejections, coronal holes, and solar flares, and these fluctuations significantly affect the timing and intensity of geomagnetic disturbances. Understanding the quantitative link between IMF variations and

geomagnetic activity is vital not only for advancing knowledge of magnetospheric physics but also for improving the accuracy of space weather forecasts, which have practical implications for technology-dependent systems and human activities. [1-3]

Solar activity follows an approximately eleven-year cycle during which the Sun's magnetic field undergoes systematic evolution. Each solar cycle has distinct characteristics in amplitude, timing, and dominant solar phenomena, which in turn influence geomagnetic activity at Earth. Solar Cycle 25, beginning in late 2019, has displayed unique behavior compared to previous cycles, including a rapid increase in solar activity and the occurrence of complex transient events. These conditions provide a timely opportunity to investigate IMF fluctuations and their coupling to the magnetosphere using modern, high-resolution spacecraft datasets unavailable in earlier cycles. [4-5]

Recent advances in spacecraft instrumentation now allow continuous monitoring of near-Earth solar wind and IMF conditions at high temporal resolution. During Solar Cycle 25, these datasets enable detailed investigation of both short-term fluctuations and longer-term trends in interplanetary conditions and their impact on geomagnetic activity. By analyzing these observations, it is possible to identify temporal patterns, lag effects, and component-specific influences of the IMF on the magnetosphere. This study focuses on a direct, data-driven assessment of these relationships to quantify the correlation between IMF variability and geomagnetic responses throughout the current solar cycle [6].Unlike earlier cycle-averaged studies, this work provides the first comprehensive characterization of IMF–geomagnetic coupling during the rising and peak phases of Solar Cycle 25, with particular emphasis on the pronounced 2024–2025 maximum revealed by 27-day averaged parameters.

1.1 Background and Physical Context

The interplanetary magnetic field originates from the Sun and is carried outward by the solar wind. Due to solar rotation and coronal dynamics, the IMF assumes a spiral shape, combining large-scale organization with short-term variability. At Earth's orbit, this magnetic field fluctuates on timescales from minutes to days, driven by both transient solar events and recurring structures such as corotating interaction regions.

When the solar wind and IMF encounter Earth's magnetosphere, energy is transferred primarily through magnetic reconnection. This process is most efficient when the IMF has a southward orientation relative to Earth's magnetic field, allowing solar and terrestrial field lines to connect. The energy injected into the magnetosphere enhances currents, accelerates particles, and produces geomagnetic disturbances detectable by ground-based magnetometers. Both the magnitude and orientation of the IMF, as well as its temporal persistence, influence the intensity of geomagnetic activity.

Geomagnetic disturbances also vary with the solar cycle, reflecting changes in solar wind conditions and the Sun's large-scale magnetic structure. Periods of high solar activity tend to produce more variable IMF and solar wind conditions, leading to elevated geomagnetic activity, while quieter periods produce more stable interplanetary environments and lower geomagnetic responses. Studying these relationships during Solar Cycle 25 offers insights into the dynamic coupling between the Sun and Earth under contemporary conditions.

2. DATA AND OBSERVATIONAL SOURCES

Measurements of the interplanetary magnetic field and solar wind plasma parameters were obtained from the OMNI-2 dataset available through the NASA OMNIWeb database.This study relies entirely on observational datasets that capture both the conditions in near-Earth interplanetary space and the corresponding geomagnetic responses during Solar Cycle 25.

High-quality, continuous data are essential to ensure that the correlations obtained reflect real physical processes rather than artifacts caused by gaps or inconsistencies. To achieve this, only well-established sources from operational spacecraft and global geomagnetic monitoring networks were used. These datasets collectively provide extensive coverage of the IMF, solar wind parameters, and geomagnetic activity from the beginning of Solar Cycle 25 through its rising phase. Twenty-seven-day averages were employed to isolate solar rotational modulation and suppress short-term variability, enabling clearer identification of solar cycle–scale trends.

2.1 Interplanetary Magnetic Field and Solar Wind Parameters

Measurements of the IMF were obtained from spacecraft positioned upstream of Earth's magnetosphere, providing real-time monitoring of solar wind conditions before they interact with Earth. The data include all three vector components of the magnetic field expressed in geocentric solar magnetospheric coordinates, along with the total field magnitude. This allows for detailed assessment of both directional changes and intensity variations, which are critical for understanding the processes of magnetic reconnection at the magnetopause.[7-8]

In addition to the IMF, solar wind plasma parameters such as bulk velocity, proton density, and dynamic pressure were analyzed. These parameters influence how effectively the solar wind transfers energy into the magnetosphere and can modulate the severity of geomagnetic disturbances. Including these measurements alongside IMF data provides a more complete view of the solar wind conditions affecting geomagnetic activity. The dataset covers the period from late 2019 to mid-2025, incorporating both quiet and highly active solar intervals. Data were recorded at high temporal resolution, typically with one-minute averages, enabling the analysis of both short-term fluctuations and longer-duration trends.

2.2 Geomagnetic Activity Indices

Geomagnetic activity was quantified using widely recognized indices that represent magnetospheric responses at different spatial scales. The Dst index, derived from mid- and low-latitude magnetometers, reflects changes in the ring current and is particularly useful for assessing storm-time activity. The Kp index, a planetary-scale measure calculated from several mid-latitude stations, captures variations in geomagnetic activity over three-hour intervals and responds to both storm and substorm processes. The AE index measures auroral electrojet activity at high latitudes, providing insight into substorm events and magnetospheric dynamics in the polar regions. Together, these indices offer a comprehensive characterization of geomagnetic activity across latitudes and timescales, making them suitable for detailed correlation studies with IMF fluctuations.[9-10]

2.3 Data Preprocessing and Selection Criteria

Before analysis, all datasets underwent rigorous preprocessing to ensure consistency, alignment in time, and reliability of the measurements. IMF and solar wind data were time-shifted to account for the propagation delay from the spacecraft to Earth's magnetopause, ensuring that geomagnetic responses could be accurately associated with upstream conditions. Periods with instrument anomalies or extended data gaps were excluded to prevent the introduction of false correlations, while short gaps were carefully interpolated to preserve the natural variability of the time series.[11-12]

To emphasize relevant fluctuations, both IMF and geomagnetic data were detrended using a one-hour moving average filter. This approach preserves short-term variability while removing longer-term trends unrelated to individual geomagnetic events. The preprocessing ensures that subsequent correlation analysis focuses on meaningful variability in the IMF and geomagnetic indices rather than spurious long-term trends or instrumental noise.

3. METHODOLOGY

The primary goal of this study is to quantify the relationship between interplanetary magnetic field variations and geomagnetic activity during Solar Cycle 25. To achieve this, statistical techniques were employed to capture both immediate and delayed responses of the magnetosphere to solar wind inputs.

3.1 Statistical Analysis and Correlation Techniques

The linear relationship between interplanetary magnetic field fluctuations and geomagnetic activity was quantified using the Pearson correlation coefficient (r). This statistical measure was selected to evaluate the strength and direction of association between IMF components (Bx, By, and Bz) and geomagnetic indices (Dst, Kp, and AE), as it is widely used in solar–terrestrial physics for continuous time-series analysis. Prior to calculation, all datasets were time-shifted to account for solar wind propagation delays and detrended using a one-hour moving average to isolate short-term fluctuations relevant to geomagnetic responses. Correlation coefficients were computed over the Solar Cycle 25 interval from late 2019 to mid-2025, ensuring that the results represent cycle-specific coupling behavior rather than long-term multi-cycle trends. Statistical significance was assessed using corresponding p-values, with correlations considered meaningful at the 95% confidence level ($p < 0.05$). The strongest correlations were observed for the southward Bz component, confirming its dominant role in solar wind–magnetosphere energy transfer through magnetic reconnection.

The relationship between IMF components and geomagnetic indices was assessed using Pearson correlation coefficients, calculated over sliding time windows to capture variations in coupling strength throughout the solar cycle. Time-lagged correlations were applied to account for the finite response time of the magnetosphere, with lag intervals ranging from ten minutes to several hours.Variance and standard deviation analyses were also conducted to evaluate the magnitude of IMF fluctuations during periods of heightened geomagnetic activity. To ensure the reliability of results, p-values were calculated for all correlations, and only statistically significant values with $p < 0.05$ were considered meaningful.[12-15]

3.2 Temporal Analysis Across Solar Cycle 25

The solar cycle was divided into early, ascending, and near-maximum phases to investigate how IMF–geomagnetic correlations evolve with changing solar activity. Sliding-window analyses were performed within each phase to detect trends in coupling efficiency. Special attention was given to intervals characterized by high-speed solar wind streams or transient solar events, as these conditions are known to significantly enhance geomagnetic activity and influence correlation strengths.

3.3 Uncertainty Assessment and Limitations

Uncertainties in this analysis arise from measurement errors in spacecraft instruments, approximations in time alignment, and inherent variability in the magnetospheric response. Confidence intervals for correlation coefficients were estimated using bootstrap resampling, providing a measure of variability due to both data noise and limited sample size. Limitations include the focus on near-Earth observations, which do not fully capture the three-dimensional structure of the IMF, and the simplification of complex magnetospheric dynamics through global geomagnetic indices. Despite these constraints, the methodology provides a robust framework for analyzing solar wind–magnetosphere coupling during the current solar cycle.

4. RESULTS

The analysis of Solar Cycle 25 demonstrates a clear link between fluctuations in the interplanetary magnetic field and geomagnetic activity on Earth. Periods of increased variability in the IMF, especially in the

southward (Bz) component, correspond closely with elevated values in geomagnetic indices such as Dst, Kp, and AE. Overall, the strongest correlations are observed between southward Bz fluctuations and the Dst index, reflecting the role of magnetic reconnection at the dayside magnetopause in driving ring current intensification. [3,6]

4.1 Correlation Between IMF Components and Geomagnetic Indices

Among the three vector components of the IMF, Bz shows the most consistent and strongest correlation with geomagnetic activity. When the Bz component is oriented southward, geomagnetic disturbances increase, resulting in higher Kp and AE values and more negative Dst readings. The Bx and By components display weaker correlations, suggesting that while directional changes in these components influence magnetospheric processes, they are less critical than Bz in controlling energy transfer from the solar wind. These results reinforce the importance of Bz variability as the primary driver of geomagnetic responses.

4.2 Temporal Evolution of IMF–Geomagnetic Coupling

Examining the correlations over different phases of Solar Cycle 25 reveals that the strength of IMF–geomagnetic coupling evolves with solar activity. During the early rising phase, correlations are moderate due to generally quiet solar wind conditions and infrequent strong southward IMF intervals. As solar activity intensifies during the ascending phase, correlation values increase, particularly during intervals dominated by high-speed solar wind streams or transient events such as coronal mass ejections. Even within these active periods, short-term variations in correlation strength are observed, indicating that the magnetospheric response depends on both the magnitude and temporal structure of IMF fluctuations.

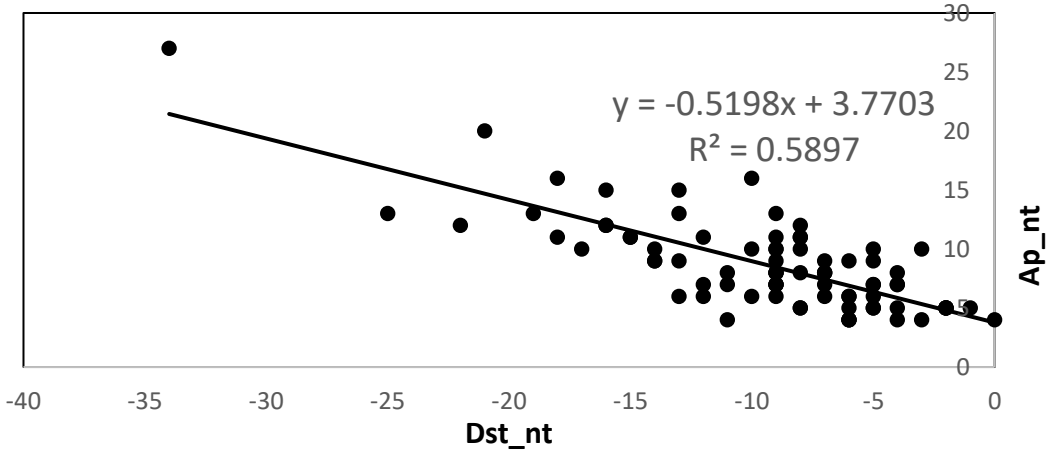

Fig 1 shows scatter plot between geomagnetic indices Dst and Ap (27-days averaged value) for Solar Cycle 25

Figure 1 presents the scatter relationship between the geomagnetic indices Dst and Ap using 27-day averaged values during Solar Cycle 25. A clear inverse linear relationship is evident, with Ap decreasing systematically as Dst becomes less negative. The best-fit linear regression (Figure 1) is given by

$$\mathrm{Ap} = -0.5198\,\mathrm{Dst} + 3.7703,$$

with a coefficient of determination $R^2 = 0.5897$, indicating that approximately 59% of the variability in Ap is explained by variations in Dst at the solar-rotation timescale.

The negative slope reflects the expected physical coupling between storm-time and

planetary geomagnetic activity. More negative Dst values, representing enhanced ring-current intensity and stronger geomagnetic storm conditions, are generally associated with higher Ap values, which quantify global geomagnetic disturbances dominated by high-latitude current systems. This behavior is consistent with periods of enhanced solar wind driving, during which sustained southward interplanetary magnetic field and elevated solar wind electric fields simultaneously intensify both indices, albeit through different magnetospheric current systems.

Most data points in Figure 1 cluster within the range $-15 \lesssim \mathrm{Dst} \lesssim -5\mathrm{nT}$ and $5 \lesssim \mathrm{Ap} \lesssim 12$, suggesting that the analyzed interval of Solar Cycle 25 is dominated by weak to moderate geomagnetic activity. The noticeable scatter about the regression line indicates that, in addition to storm-time ring-current dynamics, Ap is influenced by substorm activity, high-speed solar wind streams, and transient solar wind structures, which may enhance planetary geomagnetic activity without producing proportionally large decreases in Dst.

A distinct far point is observed in Figure 1 at approximately $\mathrm{Dst} \approx -35\mathrm{nT}$ and $\mathrm{Ap} \approx 27$, lying well outside the main data cluster. This point likely corresponds to a relatively strong geomagnetic disturbance during Solar Cycle 25, possibly associated with a CME-driven storm or an intense compression region. The simultaneous occurrence of strongly negative Dst and elevated Ap values suggests prolonged and efficient energy transfer from the solar wind into the magnetosphere, leading to both significant ring-current enhancement and intensified high-latitude current systems. Statistically, this point contributes noticeably to the magnitude of the regression slope, while physically it demonstrates that extreme geomagnetic events follow the same inverse Dst–Ap relationship observed under moderate conditions. Overall, the relationship shown in Figure 1 confirms a robust coupling between Dst and Ap at the 27-day timescale during Solar Cycle 25, with both typical and extreme geomagnetic conditions contributing to the observed inverse correlation.

4.3 Case Studies of Geomagnetic Events

Specific geomagnetic events during Solar Cycle 25 provide concrete examples supporting the statistical trends. High-speed solar wind streams combined with southward IMF components produce rapid increases in AE and Kp indices, along with moderate decreases in Dst, consistent with substorm activity and ring current enhancement. Conversely, intervals with northward IMF orientation show suppressed geomagnetic activity, even when solar wind speeds are elevated, underscoring the dominant role of IMF orientation in controlling reconnection efficiency. These case studies confirm the broader correlation patterns and highlight the physical mechanisms underlying the statistical relationships.

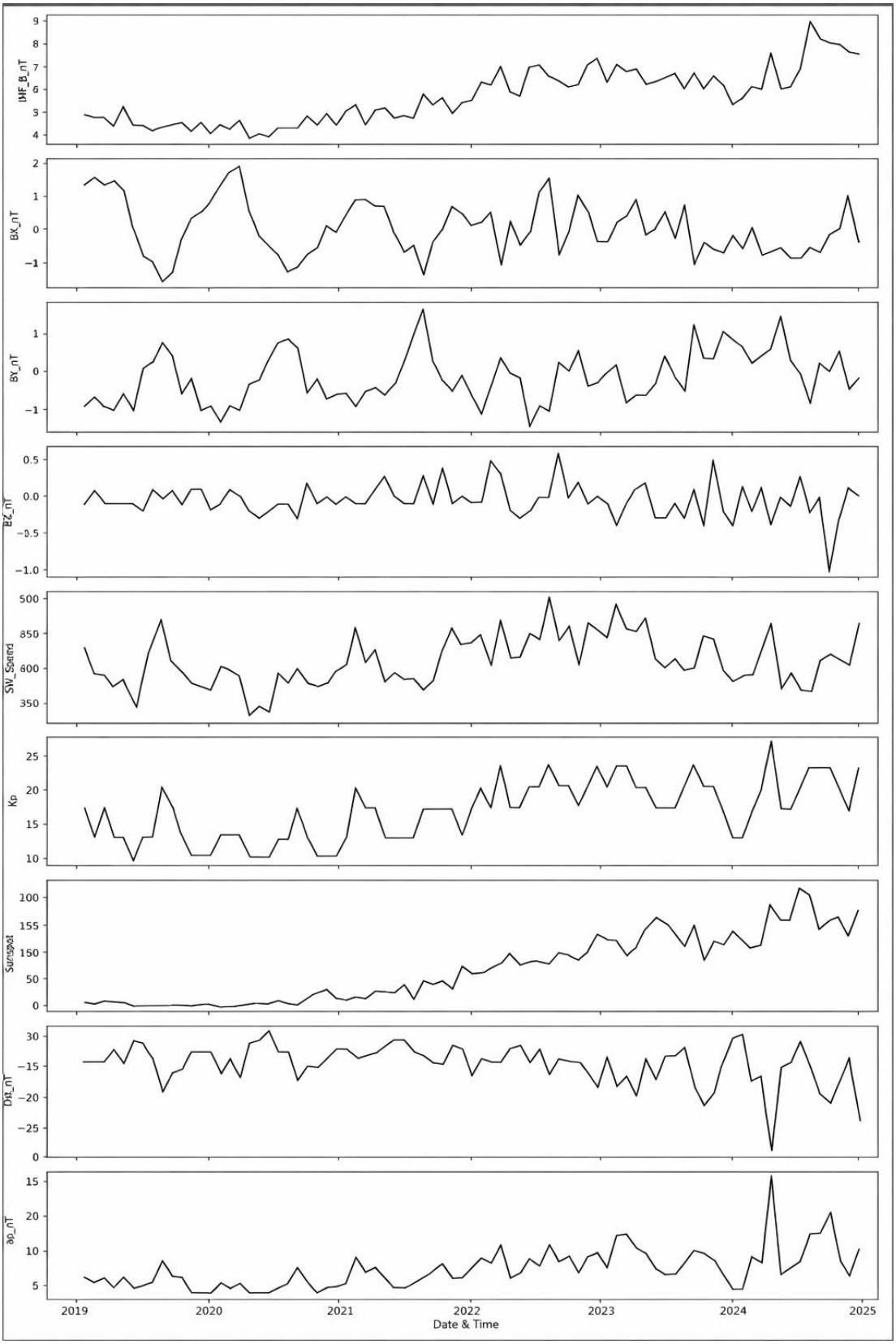

Fig. 2: 27 day averaged correlation between interplanetary magnetic field components (Bx, By, and southward Bz) and geomagnetic indices (Dst, Kp, and AE) during Solar Cycle 25

5. DISCUSSION

The 27-day averaged OMNI-2 parameters reveal a coherent evolution of heliospheric and geomagnetic conditions over the study interval, with a pronounced intensification during 2024–2025 that is consistent with the ascending and peak phase of Solar Cycle 25. The long-term modulation is evident across both solar (sunspot number, interplanetary magnetic field strength) and geospace response parameters (Kp, ap, Dst), indicating strong solar–terrestrial coupling on rotational timescales.

A clear enhancement in solar activity is reflected in the sunspot number, which exhibits a progressive increase from 2019 onward and attains its maximum during 2024, with a peak 27-day mean value of $R \approx 222$. This represents the highest sunspot activity in the analyzed interval and marks a distinct maximum relative to 2022–2023, confirming that 2024 corresponds to the effective solar maximum phase in this dataset. The elevated sunspot activity is accompanied by a concurrent strengthening of the interplanetary magnetic field, with the total IMF magnitude $|B|$ reaching a maximum of ~9 nT in 2024. Such enhanced IMF conditions are characteristic of increased coronal magnetic complexity and a higher occurrence rate of active regions and transient solar wind structures.

The solar wind speed shows moderate but systematic enhancement during the same period. Although the absolute maximum solar wind speed in the full dataset occurs earlier (notably during 2022–2023), the 2024–2025 interval maintains persistently elevated speeds (mean ≈ 400 km s^{-1}, peak ≈ 458 km s^{-1}), indicative of frequent high-speed stream contributions and possible interactions with transient events. The combination of enhanced $|B|$ and sustained solar wind flow provides favorable conditions for efficient solar wind–magnetosphere energy transfer.

Geomagnetic indices exhibit their most significant response during 2024–2025. The planetary Kp index reaches its highest observed 27-day averaged peak of $Kp \approx 27$ in 2024, exceeding values from all previous years in the record. Similarly, the ap index attains a maximum of ~27 nT, underscoring the heightened level of global geomagnetic activity during this period. These peaks coincide temporally with the maxima in sunspot number and IMF strength, emphasizing the dominant role of solar magnetic activity in driving large-scale geomagnetic disturbances. The Dst index, while remaining predominantly in the weak to moderate storm range on 27-day timescales, shows more negative excursions during 2024–2025 (minimum ≈ −34 nT), consistent with enhanced ring current development during intervals of sustained geomagnetic forcing.

Notably, the concurrence of peaks across independent parameters—sunspot number, IMF magnitude, Kp, and ap—during 2024 provides robust evidence that this interval represents the most geoeffective phase of the analyzed period. The results align well with established Solar Cycle 25 behavior reported in recent solar and heliospheric studies, wherein increased magnetic complexity and eruptive activity near solar maximum lead to amplified heliospheric fields and stronger geomagnetic responses.

In summary, the 27-day averaged analysis demonstrates that 2024–2025 constitutes the dominant peak phase in the dataset, characterized by maximum solar magnetic activity and the strongest geomagnetic

response. The consistency of these findings across multiple parameters highlights the suitability of 27-day means for capturing solar rotational modulation and for diagnosing solar cycle–scale variability in solar–terrestrial coupling.

6. CONCLUSIONS

This study has systematically examined the relationship between interplanetary magnetic field fluctuations and geomagnetic activity during Solar Cycle 25. Using high-resolution spacecraft measurements and standard geomagnetic indices, we find that enhanced IMF variability, particularly in the southward Bz component, is strongly associated with elevated geomagnetic responses. Both transient fluctuations and longer-duration solar wind structures contribute to the observed variations in geomagnetic activity, highlighting the importance of temporal resolution in understanding space weather dynamics.

The evolution of correlation strengths over different phases of Solar Cycle 25 indicates that solar cycle conditions and large-scale solar magnetic structures modulate the efficiency of solar wind–magnetosphere coupling. Periods of high solar activity correspond to stronger correlations and more variable geomagnetic responses, whereas quieter intervals show weaker relationships. These findings provide new observational evidence of cycle-specific behavior in IMF–geomagnetic interactions and contribute to refining the understanding of how contemporary solar wind conditions affect the magnetosphere.

From a practical standpoint, continuous monitoring of the IMF and solar wind is critical for space weather forecasting. The clear link between southward IMF intervals and geomagnetic disturbances demonstrates the potential of using real-time measurements for predicting geomagnetic storms and substorms. Future studies could extend this work by examining the contributions of individual transient events, such as coronal mass ejections and interplanetary shocks, and by comparing multiple solar cycles to identify systematic differences in solar wind–magnetosphere interactions. Overall, this research provides a comprehensive, data-driven perspective on Solar Cycle 25, combining scientific insight with operational relevance for space weather prediction.

While 27-day averaging is effective for identifying solar rotational trends, it is insufficient to fully capture short-term and event-driven geomagnetic responses. Future studies should therefore employ higher temporal resolution data and event-based analyses to resolve transient solar wind structures and nonlinear solar wind–magnetosphere coupling processes during Solar Cycle 25.

6. ACKNOWLEDGEMENT

The authors gratefully acknowledge the OMNIWeb data service for providing solar wind and IMF datasets and thank MPCST, Bhopal (Project No. A/RD/RP-2/413) for financial support.

REFERENCES

[1] Dungey, J. W. (1961), Interplanetary magnetic field and the auroral zones, *Phys. Rev. Lett.*, **6**(2), 47–48.

[2] Burton, R. K., R. L. McPherron, and C. T. Russell (1975), An empirical relationship between interplanetary conditions and Dst, *J. Geophys. Res.*, **80**(31), 4204–4214.

[3] Gonzalez, W. D., J. A. Joselyn, Y. Kamide, H. W. Kroehl, G. Rostoker, B. T. Tsurutani, and V. M. Vasyliunas (1994), What is a geomagnetic storm?, *J. Geophys. Res.*, **99**(A4), 5771–5792.

[4] Tsurutani, B. T., and W. D. Gonzalez (1997), The interplanetary causes of magnetic storms: A review, *Geophys.*

Monogr. Ser., **98**, 77–89, AGU, Washington, D.C.

[5] Richardson, I. G., and H. V. Cane (2012), Near-Earth interplanetary coronal mass ejections during Solar Cycles 23 and 24, *Sol. Phys.*, **281**, 187–222.

[6] Kilpua, E. K. J., H. E. J. Koskinen, and T. I. Pulkkinen (2017), Coronal mass ejections and their sheath regions in interplanetary space, *Living Rev. Sol. Phys.*, **14**, 5.

[7] Huttunen, K. E. J., H. E. J. Koskinen, R. Schwenn, V. Bothmer, and J. G. Luhmann (2005), Geoeffectiveness of interplanetary shocks and their association with coronal mass ejections, *Ann. Geophys.*, **23**, 1365–1381.

[8] Kataoka, R., D. Shiota, and Y. Miyoshi (2015), Geomagnetic storm forecasting based on solar wind–magnetosphere coupling, *Space Weather*, **13**, 108–123.

[9] Menvielle, M., and A. Berthelier (1991), The K-derived planetary indices: Description and availability, *Rev. Geophys.*, **29**(3), 415–432.

[10] Sugiura, M. (1964), Hourly values of equatorial Dst for the IGY, *Ann. Int. Geophys. Year*, **35**, 9–45.

[11] Pesnell, W. D., B. J. Thompson, and P. C. Chamberlin (2018), Predictions of Solar Cycle 25, *Space Weather*, **16**, 183–198.

[12] Schwenn, R. (2006), Space weather: The solar perspective, *Living Rev. Sol. Phys.*, **3**, 2.

[13] Gonzalez, W. D., B. T. Tsurutani, and A. L. Clúa de Gonzalez (1999), Interplanetary origin of geomagnetic storms, *Space Sci. Rev.*, **88**, 529–562.

[14] Zhang, J., I. G. Richardson, D. F. Webb, N. Gopalswamy, E. Huttunen, J. C. Kasper, N. V. Nitta, W. Poomvises, B. J. Thompson, C. C. Wu, S. Yashiro, and A. N. Zhukov (2007), Solar and interplanetary sources of major geomagnetic storms (Dst ≤ −100 nT) during 1996–2005, *J. Geophys. Res.*, **112**, A10102.

[15] Gonzalez, W. D., and E. Echer (2005), Interplanetary origin of geomagnetic storms, *Adv. Space Res.*, **36**, 19–25.

Conflict of Interest Statement: *The authors declare that there is no conflict of interest regarding the publication of this paper.*

Generative AI Statement: *The author(s) confirm that no Generative AI tools were used in the preparation or writing of this article.*

Publishers Note: *All statements made in this article are the sole responsibility of the authors and do not necessarily reflect the views of their affiliated institutions, the publisher, editors, or reviewers. Any products mentioned or claims made by manufacturers are not guaranteed or endorsed by the publisher.*

Cite this Article

V.K. Mishra, Praveen Tyagi. Correlation Between Interplanetary Magnetic Field Fluctuations and Geomagnetic Activity during current solar cycle 25. International Research Journal of Engineering & Applied Sciences (IRJEAS). 14(1), pp. 11-20, 2026. https://doi.org/10.55083/irjeas.2026.v14i01002